Bioorganic & Medicinal Chemistry Letters xxx (2016) xxx–xxx

Contents lists available at ScienceDirect

Bioorganic & Medicinal Chemistry Letters

journal homepage: www.elsevier.com/locate/bmcl

Quinoxaline-based inhibitors of Ebola and Marburg VP40 egress

H. Marie Loughran [a], Ziying Han [b], Jay E. Wrobel [a,*], Sarah E. Decker [a], Gordon Ruthel [b], Bruce D. Freedman [b], Ronald N. Harty [b], Allen B. Reitz [a]

[a] Fox Chase Chemical Diversity Center, Inc, 3805 Old Easton Road, Doylestown, PA 18902, United States
[b] Department of Pathobiology, School of Veterinary Medicine, University of Pennsylvania, Philadelphia, PA 19104, United States

ARTICLE INFO

Article history:
Received 13 May 2016
Revised 17 June 2016
Accepted 18 June 2016
Available online xxxx

Keywords:
Ebola virus
Marburg virus
RNA viruses
Virus egress
PPxY
Nedd4
L-domain
Budding
Antiviral therapeutic

ABSTRACT

We prepared a series of quinoxalin-2-mercapto-acetyl-urea analogs and evaluated them for their ability to inhibit viral egress in our Marburg and Ebola VP40 VLP budding assays in HEK293T cells. We also evaluated selected compounds in our bimolecular complementation assay (BiMC) to detect and visualize a Marburg mVP40–Nedd4 interaction in live mammalian cells. Antiviral activity was assessed for selected compounds using a live recombinant vesicular stomatitis virus (VSV) (M40 virus) that expresses the EBOV VP40 PPxY L-domain. Finally selected compounds were evaluated in several ADME assays to have an early assessment of their drug properties. Our compounds had low nM potency in these assays (e.g., compounds **21**, **24**, **26**, **39**), and had good human liver microsome stability, as well as little or no inhibition of P450 3A4.

© 2016 Elsevier Ltd. All rights reserved.

The 2014–2015 outbreak of Ebola in western Africa resulted in over 28,000 infected individuals and over 11,000 deaths (WHO: Ebola situation report 2015). This unprecedented epidemic has spurred a call to action on new, cost effective therapies that combat this deadly pathogen. Among the efforts are several vaccines and antiviral candidates.[1–3] However the current vaccines in clinical trials are not a complete defense. They must be given pre-exposure and would not be effective against other RNA viruses such as Marburg and Lassa[4] that also cause lethal hemorrhagic fever symptoms. Furthermore, oral antiviral agents used alone or in combination may be of value for individuals who respond adversely to the vaccine, and could be of value as prophylactic agents for individuals deemed to be in high risk situations such as military or healthcare workers. Therefore, effective therapeutics are needed to safeguard the largely immunologically naive human population by providing immediate protection.

We have discovered two novel series of small molecule early leads that inhibit RNA virus budding.[5] Our approach does not rely solely on viral targets, but instead focuses on a critical virus-host interaction required by PPxY motif-containing viruses for efficient egress and spread. We hypothesize that targeting a virus–host interaction necessary for efficient virus egress and dissemination will greatly diminish or eliminate the occurrence of drug resistant viral mutations. Importantly, as these virus-host interactions represent a common mechanism in a range of RNA viruses, we predict that they represent an Achilles' heel in the life cycle of RNA virus pathogens.

Late budding domains (containing PPxY and PTAP motifs) are highly conserved in the matrix proteins of a wide array of RNA viruses (e.g., filoviruses, arenaviruses, rhabdoviruses, paramyxoviruses, henipaviruses, and retroviruses) and represent broad-spectrum targets for the development of novel antiviral therapeutics.[6–16] For example, the filovirus VP40, arenavirus Z, and rhabdovirus M proteins play central and sufficient roles in virion assembly and egress, due in part to the presence of a PPxY L-domain.[16–23] Efficient egress of VLPs depends on viral L-domain mediated recruitment of host proteins required for complete virus-cell separation or pinching-off of virus particles.[7–9,11–13,15,16,24] In this regard, the viral matrix protein VP40 (for filoviruses Ebola and Marburg) or Z (for arenavirus Lassa) contains a PPxY L-domain motif that recruits the mammalian cellular protein Nedd4, which is a WW-domain containing cellular E3 ubiquitin ligase associated with the host ESCRT1 complex (endosomal sorting complex required for transport), and this interaction is critical for efficient budding of filoviruses, arenaviruses, and rhabdoviruses.[9,11,15,16,18,22,24–34]

* Corresponding author.

http://dx.doi.org/10.1016/j.bmcl.2016.06.053
0960-894X/© 2016 Elsevier Ltd. All rights reserved.

Herein we describe our current efforts to exploit the viral PPxY–host WW domain interaction to obtain broad-spectrum RNA antiviral therapeutics. This paper focuses on SAR around our lead **1** (Table 1) which we described in detail previously.[5] We used our Marburg VP40 VLP budding assay in HEK293T cells as our primary assay for the SAR analogs compiled in Tables 1–3. This assay measures the % inhibition of viral VP40 VLP egress from the cell versus DMSO control. In addition we provide Western analysis for selected compounds using this assay and the Ebola VP40 VLP budding assay (Figs. 2 and 3). We also evaluated selected compounds in our bimolecular complementation assay (BiMC)[35] to detect and visualize a Marburg VP40–Nedd4 interaction in live mammalian cells in the absence or presence of the indicated inhibitors in Figure 1. We then assessed antiviral activity for selected compounds using a live recombinant vesicular stomatitis virus (VSV-M40 virus) that expresses the EBOV VP40 PPxY L-domain and flanking residues[36] in Figure 4. Relative cell viability was validated by the MTT assay at concentration ranges of 0.01–1.0 μM on VeroE6 and HEK293T cells (data presented in Supplementary material section). Finally selected compounds were evaluated in several ADME assays (Table 4) to have an early assessment of their drug properties.

Compounds **2**–**13** (Table 1) and **17**–**52** (Tables 2 and 3) were prepared according to Schemes 1 and 2. While compounds **1** and **14**–**16** were originally purchased from Ambinter (Orléans, France), larger quantities of **1** were synthesized by us via the methods outlined in Scheme 1. Experimental and analytical information for compounds **1**–**13** and **17**–**52** are described in the Supplementary material section.

Referring to Scheme 1, target compounds in Tables 1–3 were generally prepared by alkylation of quinoxaline thiols **55** with α-chloro-acetamidoureas **57**. The alkylating agents (**57**) were in turn obtained via reaction of commercially available anilines or heteroaromatic amines **56** with commercially available chloroacetyl isocyanate. In most cases, the quinoxaline thiol **55** was commercially available but in a few examples ($R^1 = CF_3$ and Et) we prepared this thiol by converting congeners **54** ($R^1 = CF_3$ and Et) using P_2S_5 and pyridine.[37] Compound **54** where $R^1 = CF_3$ was prepared by reaction of *o*-phenylenediamine with ethyl trifluoropyruvate[38] and **54** where R^1 = Et is commercially available.

Several of the target compounds in Table 1 were prepared by alternative routes highlighted in Scheme 2. For compounds with X = O (e.g., **9** and **10**), we started with commercially available 2-chloro-3-methyl-quinoxaline (**58**) since reaction of compounds **54** with **57** led to N-alkylation products. Substitution of the chlorine of **58** with methyl glycolate, and subsequent saponification of the methyl ester led to acid **59**. Conversion to the primary amide **60** and subsequent reaction with the requisite aryl isocyanate[39,40] led to target compounds **9** and **10**. Preparation of *N*-methylated target compound **12** ($R^2 = CH_3$) was accomplished by alkylation of **20** with methyl iodide. Thioether **20** was also used to prepare sulfone analog **8** via mCPBA oxidation conditions.

We examined the X and R^1–R^3 substituent changes of **1** in Table 1. With the exception of analogs **9** and **10**, the compounds **2**–**8**, **11**–**13** in this table had little or no inhibition of Marburg VLP egress at 1 μM or greater. SAR highlights are summarized below with the full data set listed in the Supplementary section (Table 1S). Tables 2 and 3 focused on variation of the terminal aryl substituent of **1**.

Referring to Table 1, we have not found a suitable replacement of methyl for the **R^1** substituent on the quinoxaline moiety of **1**. All replacements either smaller, H (**2**) or larger, CF_3 (**3**, **4**), Et (**5**, **6**) or CH_2Ph (**7**) were less active or not active at the 1 μM concentration in the Marburg VLP inhibition assay. The CF_3 and Et groups did provide compounds with greater stability to mouse liver microsomes relative to the methyl congeners however (vide infra).

We replaced the sulfur atom of compound **1** (**X** = S) with a SO_2 moiety (**8**) or an O atom (**9**, **10**). While compound **8** did not show activity at 1 μM, the ether analogs **9** and **10** were approximately a

Table 1
Analogs of **1**. Examination of changes in highlighted areas

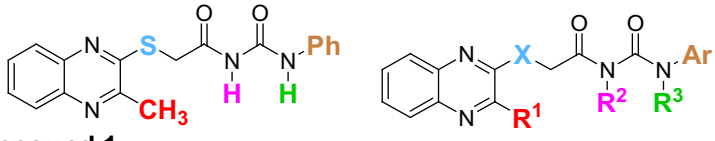

Compound 1

No.	R^1	X	R^2	R^3	Ar
2	H	S	H	H	
3	CF_3	S	H	H	
4	CF_3	S	H	H	
5	Et	S	H	H	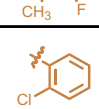
6	Et	S	H	H	
7	CH_2Ph	S	H	H	

No.	R^1	X	R^2	R^3	Ar
8	CH_3	SO_2	H	H	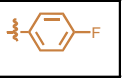
9	CH_3	O	H	H	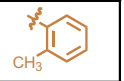
10	CH_3	O	H	H	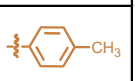
11	CH_3	S	H	CH_3	
12	CH_3	S	CH_3	H	
13	CH_3	S	H	NR^3Ar =	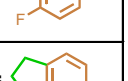

Table 2
SAR of terminal phenyl moiety of **1** with alkyl, benzyl and substituted phenyl groups

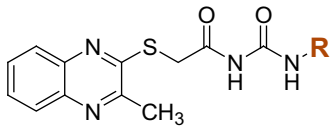

No.	R	MW	Log*D* (pH 7.4)	TPSA (Å^2)	mVLP[a] (% reduction at given concentration in μM)			
					1	0.3	0.1	0.03
1	Phenyl	352.4	2.9	84	88[b]			
14	Ethyl	316.4	1.4	84	NS[c]		NS	
15	Cyclopropyl	352.4	2.9	84	NS[d]		NS	
16	CH_2-(2)-thiophenyl	372.5	2.5	84	97		NS	
17	Benzyl	366.4	2.6	84	60		29	
18	2-Fluorophenyl	370.4	3.1	84	100	100	98	NS
19	3-Fluorophenyl	370.4	3.1	84	41			
20	4-Fluorophenyl	370.4	3.1	84	80			
21	2-Chlorophenyl	386.9	3.5	84			99[e]	93[e]
22	3-Chlorophenyl	386.9	3.5	84		49		
23	4-Chlorophenyl	386.9	3.5	84			82	
24	2-Methylphenyl	366.4	3.4	84	100		98[f]	83[f]
25	3-Methylphenyl	366.4	3.4	84	100	71	NS	NS
26	4-Methylphenyl	366.4	3.4	84	100	100	100	93
27	2-Cyanophenyl	377.4	2.8	108	87			
28	3-Cyanophenyl	377.4	2.8	108	72			
29	2-Methoxyphenyl	382.4	2.8	93	96	89	60	NS
30	3-Methoxyphenyl	382.4	2.8	93	100	98	60	NS
31	4-Methoxyphenyl	382.4	2.8	93	100		99	25
32	2,3-Dimethylphenyl	380.5	3.9	84		98		41
33	2,4-Dimethylphenyl	380.5	3.9	84		100		62
34	2,5-Dimethylphenyl	380.5	3.9	84		100		68
35	2,6-Dimethylphenyl	380.5	3.9	84		100		NS
36	3,4-Dimethylphenyl	380.5	3.9	84		97		29
37	3,5-Dimethylphenyl	380.5	3.9	84		100		44
38	2,5-Dichlorophenyl	421.3	4.1	84				37
39	3-Fluoro-2-methylphenyl	384.4	3.6	84			100[f]	86[f]
40	5-Fluoro-2-methylphenyl	384.4	3.6	84			89	

[a] Marburg VP40 VLP budding assay. HEK293T cells, NS: not significant versus DMSO control, a blank entry means the compound was not evaluated at the corresponding concentration.
[b] Average of twenty independent experiments at 1.0 μM.
[c] 60% reduction at 25 μM.
[d] 60% reduction at 10 μM.
[e] Average of two independent experiments at 0.1 and 0.03 μM concd.
[f] Average of four independent experiments at 0.1 and 0.03 μM concd.

half log less potent than their corresponding thioether analogs **24** and **26** respectively (Table 2) and showed good inhibitory activity at the 100 nM level (e.g., **9** showed 58% reduction of mVLPs at 100 nM and **10** showed 70% reduction of mVLPs at 100 nM). Other general SAR results from the compounds in Table 1 reveal that methyl substituents in place of H on the imido ($\mathbf{R^2}$) and amide ($\mathbf{R^3}$) nitrogen atoms resulted in greatly reduced activity (compounds **11** and **12** respectively) and that the amide substituent $\mathbf{R^3}$ and **Ar** moiety could not be tied back in a ring (compound **13**).

Analogs that varied the phenyl moiety of **1** with alkyl and aralkyl groups as well as the substituents on the terminal phenyl group of **1** are shown in Table 2 with their corresponding Marburg VLP assay data. Replacement of the phenyl moiety of **1** with alkyl (**14**, **15**) or aralkyl groups (**16**, **17**) did not lead to improved potency consistent with previous findings.[5] However substituent additions on the phenyl group of **1** led to many compounds with improved potency. Examination of Table 2 reveals that halo and methyl substituents particularly at the ortho and para positions [see **21** (2-Cl), **24** (2-Me) and **26** (4-Me)] showed strong activity at the lowest concentration tested (30 nM). Compounds with either strong electron releasing moieties (e.g., methoxy at o, m or p positions: compounds **29**–**31**) or strong electron withdrawing groups (e.g., cyano at *o*, *m* positions: compounds **27**, **28**) did not generally result in improved potency over **1**.

Addition of a second methyl group on the terminal phenyl ring as for compounds **32**–**37**, did not further improve potency over monomethyl congeners **24** and **26** and this was also true of the dichloro analog **38** when compared to mono-chloro analog **21**. The compound with a combination of a 2-methyl and 3-fluoro group (**39**) did show strong potency however.

Replacement of the terminal phenyl group or **1** with a heteroaromatic moiety is shown in Table 3. Thus far unsubstituted and methyl/alkyl substituted 2-pyridyl (**41**–**44**), unsubstituted and methyl substituted 3-pyridyl (**45**–**48**) and unsubstituted and substituted pyrazole (**49**–**52**) have been investigated. The mVLP activity is presented in the Supplementary section as Table 2S. Generally these heterocyclic replacement compounds have not led to improved potency increases over **1**. A few exceptions are 2-pyridyl analog **43** and 3-pyridyl analogs **47** and **48** (96%, 85% and 87% reduction in mVLP levels at 100 nM, respectively), however these did not achieve the same magnitude of potency increases as seen by several of the substituted phenyl analogs of Table 2.

Our compounds have in silico properties (MW, *c*Log*D*, TPSA in Tables 2) that are consistent with drugs delivered orally.[41] We evaluated a few of the more potent analogs in several ADMET assays (Table 4) for a preliminary assessment of metabolic stability to liver microsomes and inhibition of P450 3A4. The compounds

Table 3
Analogs of **1**. Replace terminal phenyl moiety with heteroaromatic groups

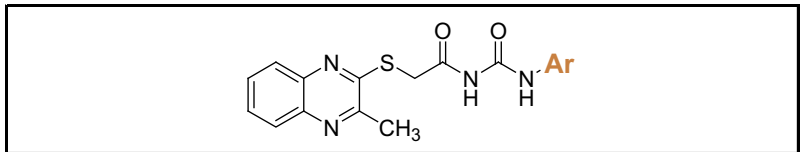

No.	Ar	No.	Ar	No.	Ar
41	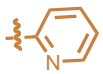	45	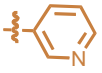	49	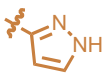
42	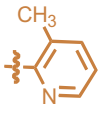	46	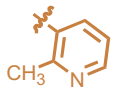	50	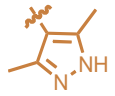
43	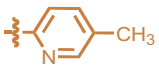	47	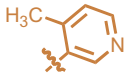	51	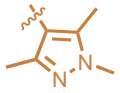
44	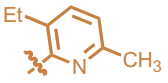	48	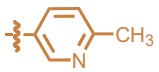	52	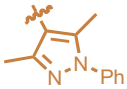

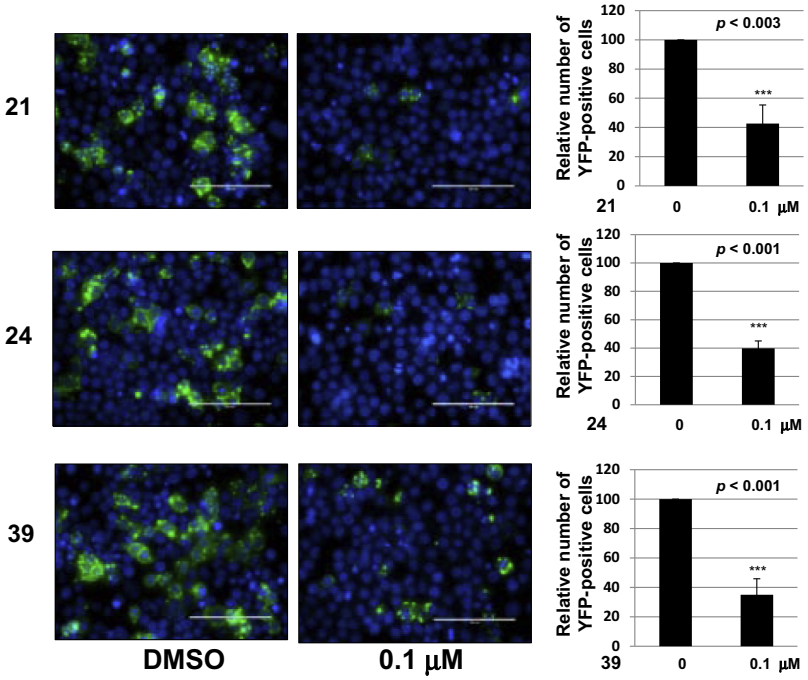

Figure 1. BiMC analysis of HEK293T cells co-expressing NYFP–Nedd4 and CYFP–mVP40 in the presence of DMSO alone, or 0.1 µM concentration of **21**, **24** or **39**. Representative images are shown where the total number of cells were quantified using NucBlue, and Green (YFP) indicates cells with a positive interaction between Nedd4 and mVP40. Scale bar, 200 µm. YFP-positive cells were quantified in triplicate using MetaMorph software and statistical analysis as described previously.[1]

generally had moderate to good stability against human liver microsomes, but the 3-methyl quinoxaline analogs **21**, **24**, **26**, **34** and **39** had poor stability against mouse liver microsomes. Since our early antiviral animal model is the mouse, we needed to improve stability in the mouse. This was indeed achieved by replacing the quinoxaline 3-methyl moiety with either a trifluromethyl or ethyl group (compounds **3** and **6** respectively). Unfortunately these compounds lost significant potency, but none-the-less provided data to guide us in the preparation of more potent mouse liver microsome stable compounds. Thus far, none of

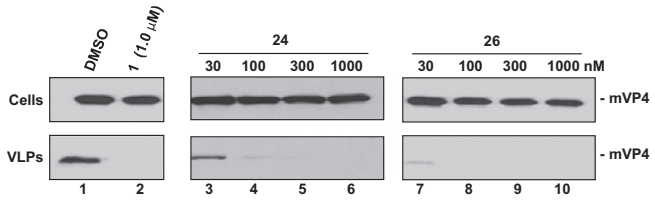

Figure 2. Marburg VP40 VLP budding assay. HEK293T cells were transfected with mVP40 plasmid in the presence of DMSO alone, or the indicated inhibitor (**24** or **26**) at the indicated concentrations. mVP40 was detected by Western blot in cell extracts and VLPs at 24 h post-transfection. mVP40 was quantified using NIH Image-J software.

our inhibitors have affected P450 3A4 activity at 33 μM, although a more stringent analysis of other P450s will have to be conducted on future analogs to best determine drug–drug interaction profiles.

We used our well established BiMC approach[35] to detect and visualize a Marburg VP40–Nedd4 interaction in live mammalian cells in the absence or presence of the indicated egress inhibitors (Fig. 1). Briefly, HEK293T cells were co-transfected with plasmids expressing NYFP–Nedd4 and CYFP–mVP40 in the presence of vehicle (DMSO) alone, or inhibitors **21**, **24**, or **39** at a concentration of 0.1 μM (Fig. 1). Total cell counts based on NucBlue staining indicated that equal numbers of cells were present in all assay samples. YFP fluorescent complementation (i.e., green cells) is indicative of a PPxY-mediated interaction between mVP40 and host Nedd4, and fluorescent cells were visualized and quantified using an inverted Leica Sp5-II confocal microscope and MetaMorph software as described previously.[5]

We observed a significant decrease in the relative number of YFP-positive cells in samples treated with either **21**, **24**, or **39** compared to that in vehicle alone control samples in multiple independent experiments. As we published previously[5], a PPxY L-domain mutant of mVP40 that does not interact with Nedd4 serves as a valid negative control (data not shown). These results demonstrate that several of our lead inhibitors can specifically block the PPxY-mediated interaction between mVP40 and Nedd4 in mammalian cells.

We used our validated filovirus VLP budding assay that recapitulates live virus budding,[11–13,15,17] to determine the antiviral potency of our analogs in Tables 1–3. We chose the Marburg mVP40 VLP budding assay as our primary screen because efficient egress of mVP40 VLPs is dependent on a single PPxY L-domain motif to recruit host Nedd4 unlike Ebola eVP40 which contains both a PTAP and PPxY motif. Figure 2 shows a pictorial example of this assay. Briefly HEK293T cells were transfected with an mVP40 expression plasmid in the presence of vehicle (DMSO) alone as a negative control, 1.0 μM **1** as a positive control, or the indicated egress inhibitors (**24** and **26**) in a dose-dependent manner. Expression levels of mVP40 were detected and quantified in cell extracts and VLPs by Western blotting and Image-J software.

As expected, budding of mVP40 VLPs was reduced by approximately 100-fold in the presence of 1.0 μM **1** compared to DMSO control (Fig. 2, lanes 1 and 2). Importantly, inhibition of budding of mVP40 VLPs was >90% in the presence of 10-fold lower (100 nM) concentrations of inhibitors **24** (Fig. 2, lane 4) and **26** (lane 8). Moreover, 30 nM concentrations of both **24** and **26** resulted in an approximately 3-fold and 15-fold decrease in mVP40 VLP budding compared to DMSO control, respectively (Fig. 2, compare lane 1 with lanes 3 and 7).

While our initial VLP budding assays employed mVP40, we have also tested several select analogs for antiviral activity against Ebola virus VP40 (eVP40) budding. While eVP40 possesses a functional PPxY-type L-domain and is thus sensitive to our PPxY budding inhibitors, it also expresses a PTAP-type L-domain that can interact with other host proteins. To determine if our compounds could block egress of both mVP40 and eVP40 VLPs, we transfected HEK293T cells with either mVP40 or eVP40 expression plasmids in the absence (DMSO alone) of inhibitor, or in the presence of **21** at the indicated concentrations (Fig. 3). Expression levels of mVP40 (red) and eVP40 (blue) were detected and quantified in cell extracts and VLPs by Western blotting and Image-J software as described previously.[5] Notably, budding of both mVP40 and eVP40 VLPs was reduced significantly at both 100 nM and 30 nM concentrations of **21** compared to that in the DMSO control

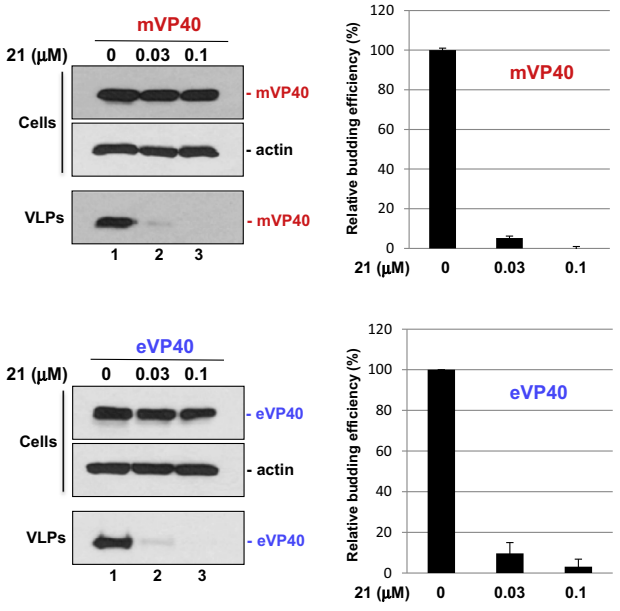

Figure 3. Marburg and Ebola VP40 VLP budding assays. HEK293T cells were transfected with either mVP40 or eVP40 plasmids in the presence of DMSO (0) alone, or budding inhibitor **21** at the indicated concentrations. mVP40 and eVP40 were detected by Western blot in cell extracts and VLPs at 24 h post-transfection. mVP40 and eVP40 were quantified using NIH Image-J software. Bar graphs represent the average of three independent experiments.

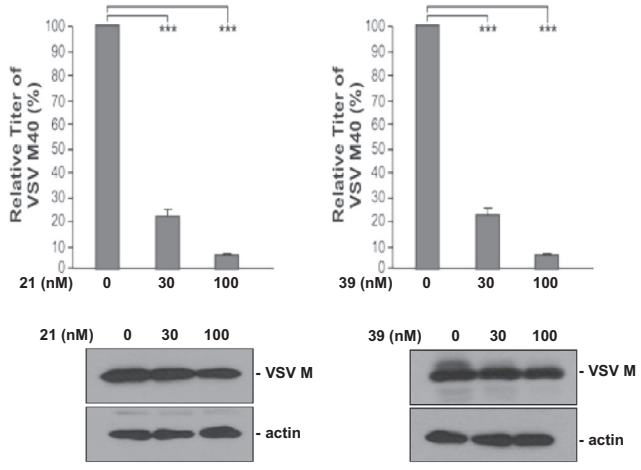

Figure 4. Inhibition of live VSV–M40 virus budding. HEK293T cells were infected (in triplicate) with VSV-M40 for 8 h under the indicated conditions, and virion containing supernatants were harvested and quantified by plaque assay performed in triplicate. Virus titers are indicated as a percent relative to control. ***Indicates a p values <0.001 as determined by a two-tailed Student t-test. Western blots of infected cell extracts are shown for VSV M and actin, which demonstrate that treatment with the indicated concentrations of **21** and **39** for 8 h did not affect viral or cellular protein levels compared to DMSO alone controls.

Table 4
ADMET data for select compounds

Compd	Microsome stability				P450 inhib IC_{50} (μM)
	Mouse		Human		
	$t_{1/2}$ (min)	Cl_{int} (mL/min/mg protein)	$t_{1/2}$ (min)	Cl_{int} (mL/min/mg protein)	3A4 (midazolam)
1	ND	ND	43.9	1.66	ND
21	2.0	34.1	76.1	0.72	>33
24	3.0	22.4	46.6	1.18	>33
26	<1.4	>50	57.7	0.95	>33
34	1.9	35.1	77.2	0.71	>33
39	3.5	18.8	>90	0.54	>33
3	49.9	1.3	71.7	0.77	>33
6	54.8	1.2	31.3	1.76	ND

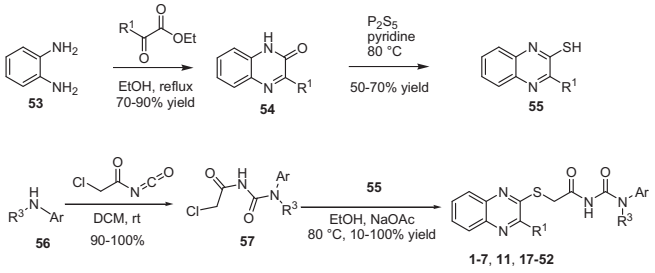

Scheme 1. General preparation of target compounds.

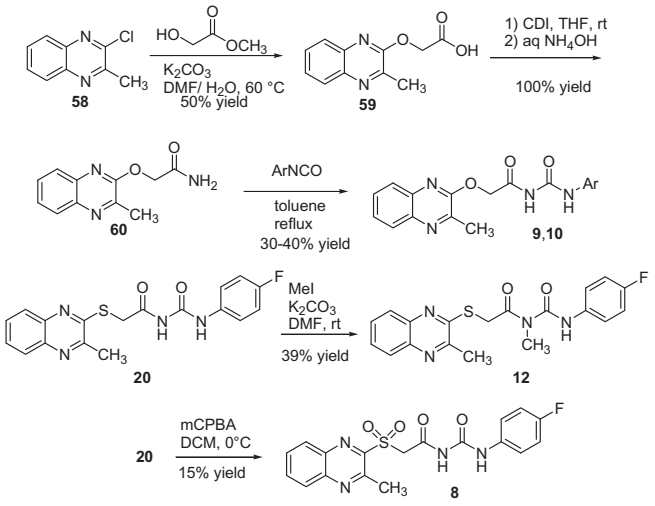

Scheme 2. Preparation of certain specific target compounds.

samples (Fig. 3). These results were consistent in multiple independent budding assays (Fig. 3, bar graphs), and highlight the enhanced antiviral potency and broad-spectrum nature of these inhibitors.

While the use of BiMC and VLP budding assays as our initial screening assays continues to be instrumental in directing us toward novel and potent budding inhibitors, the ultimate test of efficacy is their ability to inhibit infectious (live) virus budding. Toward this end, we have tested several lead candidates for their ability to block budding of VSV and/or our previously described live VSV recombinant virus (M40 virus) that expresses the eVP40 PPxY L-domain and flanking residues.[24]

Importantly, the M40-VSV recombinant virus serves as an Ebola surrogate that we can use safely under BSL-2 conditions to rapidly assess the antiviral potency of our inhibitors before having them tested with more dangerous BSL-4 pathogens (collaboration at USAMRIID). Indeed, we published recently that another egress inhibitor from different chemical series significantly decreased PPxY-mediated budding of both VSV-WT and VSV-M40.[5] Here we demonstrate that analogs **21** and **39** effectively block budding of live VSV-M40 from HEK293T cells (Fig. 4). Briefly, cells were infected with VSV-M40 at a low multiplicity of infection (MOI) of 0.1 in the presence of DMSO alone or at the indicated concentrations of **21** or **39**. Virion-containing supernatants were harvested at 8 h post-infection; the peak time for virus budding (Fig. 4). Equivalent amounts of the VSV M protein and cellular actin were detected by Western blot to demonstrate that the budding inhibitors had no detectable effects on viral protein synthesis (Fig. 4). Intriguingly, both **21** and **39** inhibited budding of VSV-M40 by approximately 5-fold at 30 nM and by >10-fold at 100 nM compared to DMSO controls in four independent experiments (Fig. 4). These findings correlate well with BiMC and VLP budding assays that demonstrate specific and potent inhibition of PPxY-mediated virus budding.

To summarize, our analogs show:

- improved potency as RNA viral egress inhibitors by >30 fold over initial lead **1** (e.g., compounds **21**, **24**, **26**, **39**);
- low nanomolar functional activity (VLP assay);
- low nM target engagement (inhibition of Nedd4/Marburg PPxY binding in cellular BiMC assay);
- inhibition of live virus egress (VSVM40);
- good human microsome stability and no inhibition of P450 3A4 at 33 μM concentration;
- little to no cytotoxicity at effective antiviral concentrations.

Live virus testing with infectious BSL-4 viruses (Ebola, Marburg, Junin, Lassa) of these and other analog series of compounds we are developing is ongoing (USAMRIID) and will be the subject of future reports.

Acknowledgments

This project was supported by National Institutes of Health (NIH): National Institute of Allergy and Infectious Diseases (NIAID) grant R41AI113952 and AI102104. We thank C. Berry for help with statistical analysis, and D. Lyles, S. Urata, and S. Becker for generously providing reagents.

Supplementary data

Supplementary data associated with this article can be found, in the online version, at http://dx.doi.org/10.1016/j.bmcl.2016.06.053.

References and notes

1. Li, H.; Ying, T.; Yu, F.; Lu, L.; Jiang, S. *Microbes Infect.* **2015**, *17*, 109.
2. De Clercq, E. *Biochem. Pharmacol.* **2015**, *93*, 1.
3. Agnandji, S. T.; Huttner, A.; Zinser, M. E.; Njuguna, P.; Dahlke, C.; Fernandes, J. F.; Yerly, S.; Dayer, J. A.; Kraehling, V.; Kasonta, R.; Adegnika, A. A.; Altfeld, M.; Auderset, F.; Bache, E. B.; Biedenkopf, N.; Borregaard, S.; Brosnahan, J. S.; Burrow, R.; Combescure, C.; Desmeules, J.; Eickmann, M.; Fehling, S. K.; Finckh, A.; Goncalves, A. R.; Grobusch, M. P.; Hooper, J.; Jambrecina, A.; Kabwende, A. L.; Kaya, G.; Kimani, D.; Lell, B.; Lemaître, B.; Lohse, A. W.; Massinga-Loembe, M.; Matthey, A.; Mordmüller, B.; Nolting, A.; Ogwang, C.; Ramharter, M.; Schmidt-Chanasit, J.; Schmiedel, S.; Silvera, P.; Stahl, F. R.; Staines, H. M.; Strecker, T.; Stubbe, H. C.; Tsofa, B.; Zaki, S.; Fast, P.; Moorthy, V.; Kaiser, L.; Krishna, S.; Becker, S.; Kieny, M.-P.; Bejon, P.; Kremsner, P. G.; Addo, M. M.; Siegrist, C.-A. *N. Engl. J. Med.* **2015**.
4. Ogbua, O.; Ajuluchukwub, E.; Uneke, C. J. *J. Vector Borne Dis.* **2007**, *44*, 1.
5. Han, Z.; Lu, J.; Liu, Y.; Davis, B.; Lee, M. S.; Olson, M. A.; Ruthel, G.; Freedman, B. D.; Schnell, M. J.; Wrobel, J. E.; Reitz, A. B.; Harty, R. N. *J. Virol.* **2014**, *88*, 7294.
6. Adamson, C. S.; Freed, E. O. *Antiviral Res.* **2010**, *85*, 119.
7. Bieniasz, P. D. *Virology* **2006**, *344*, 55.
8. Calistri, A.; Salata, C.; Parolin, C.; Palu, G. *Rev. Med. Virol.* **2009**, *19*, 31.

9. Chen, B. J.; Lamb, R. A. *Virology* **2008**, *372*, 221.
10. Chen, H.; Liu, X.; Li, Z.; Zhan, P.; De Clercq, E. *Curr. Med. Chem.* **2010**, *17*, 750.
11. Hartlieb, B.; Weissenhorn, W. *Virology* **2006**, *344*, 64.
12. Harty, R. N. *Antiviral Res.* **2009**, *81*, 189.
13. Jasenosky, L. D.; Kawaoka, Y. *Virus Res.* **2004**, *106*, 181.
14. Jiang, Y.; Liu, X.; De Clercq, E. *Curr. Med. Chem.* **2011**, *18*, 16.
15. Liu, Y.; Harty, R. N. *Future Virol.* **2010**, *5*, 481.
16. Urata, S.; de la Torre, J. C. *Adv. Virol.* **2011**, *2011*, 180326.
17. Harty, R. N.; Brown, M. E.; Wang, G.; Huibregtse, J.; Hayes, F. P. *Proc. Natl. Acad. Sci. U.S.A.* **2000**, *97*, 13871.
18. Harty, R. N.; Paragas, J.; Sudol, M.; Palese, P. *J. Virol.* **1999**, *73*, 2921.
19. Irie, T.; Licata, J. M.; McGettigan, J. P.; Schnell, M. J.; Harty, R. N. *J. Virol.* **2004**, *78*, 2657.
20. Licata, J. M.; Simpson-Holley, M.; Wright, N. T.; Han, Z.; Paragas, J.; Harty, R. N. *J. Virol.* **2003**, *77*, 1812.
21. Urata, S.; Yasuda, J. *J. Gen. Virol.* **2010**, *91*, 228.
22. Wirblich, C.; Tan, G. S.; Papaneri, A.; Godlewski, P. J.; Orenstein, J. M.; Harty, R. N.; Schnell, M. J. *J. Virol.* **2008**, *82*, 9730.
23. Zhadina, M.; Bieniasz, P. D. *PLoS Pathog.* **2010**, *6*, e1001153.
24. Irie, T.; Licata, J. M.; Harty, R. N. *Virology* **2005**, *336*, 291.
25. Dolnik, O.; Kolesnikova, L.; Stevermann, L.; Becker, S. *J. Virol.* **2010**, *84*, 7847.
26. Martin-Serrano, J.; Zang, T.; Bieniasz, P. D. *Nat. Med.* **2001**, *7*, 1313.
27. May, E. R.; Armen, R. S.; Mannan, A. M.; Brooks, C. L. (3rd) *Proteins* **2010**, *78*, 2251.
28. Pasqual, G.; Rojek, J. M.; Masin, M.; Chatton, J. Y.; Kunz, S. *PLoS Pathog.* **2011**, *7*, e1002232.
29. Perez, M.; Craven, R. C.; de la Torre, J. C. *Proc. Natl. Acad. Sci. U.S.A.* **2003**, *100*, 12978.
30. Pornillos, O.; Alam, S. L.; Davis, D. R.; Sundquist, W. I. *Nat. Struct. Biol.* **2002**, *9*, 812.
31. Pornillos, O.; Alam, S. L.; Rich, R. L.; Myszka, D. G.; Davis, D. R.; Sundquist, W. I. *EMBO J.* **2002**, *21*, 2397.
32. Timmins, J.; Schoehn, G.; Ricard-Blum, S.; Scianimanico, S.; Vernet, T.; Ruigrok, R. W.; Weissenhorn, W. *J. Mol. Biol.* **2003**, *326*, 493.
33. Urata, S.; Noda, T.; Kawaoka, Y.; Morikawa, S.; Yokosawa, H.; Yasuda, J. *J. Virol.* **2007**, *81*, 4895.
34. Urata, S.; Noda, T.; Kawaoka, Y.; Yokosawa, H.; Yasuda, J. *J. Virol.* **2006**, *80*, 4191.
35. Liu, Y.; Lee, M. S.; Olson, M. A.; Harty, R. N. *Adv. Virol.* **2011**, *2011*.
36. Irie, T.; Licata, J. M.; Jayakar, H. R.; Whitt, M. A.; Bell, P.; Harty, R. N. *J. Virol.* **2004**, *78*, 7823.
37. Makhloufi, A.; Baitiche, M.; Merbah, M.; Benachour, D. *Synth. Commun.* **2011**, *41*, 3532.
38. Yuan, H.; Li, X.; Qu, X.; Sun, L.; Xu, W.; Tang, W. *Med. Chem. Res.* **2009**, *18*, 671.
39. Schweim, H. G. *Arch. Pharm.* **1986**, *319*, 814.
40. Hisamatsu, Y.; Shirai, N.; Ikeda, S.; Odashima, K. *Org. Lett.* **2009**, *11*, 4342.
41. Waring, M. J.; Arrowsmith, J.; Leach, A. R.; Leeson, P. D.; Mandrell, S.; Owen, R. M.; Pairaudeau, G.; Pennie, W. D.; Pickett, S. D.; Wang, J.; Wallace, O.; Weir, A. *Nat. Rev. Drug Disc.* **2015**, *14*, 475.

Please cite this article in press as: Loughran, H. M.; et al. *Bioorg. Med. Chem. Lett.* (2016), http://dx.doi.org/10.1016/j.bmcl.2016.06.053